24PM1C-05

Construction of Discontinuous Galerkin Time Domain methods for Maxwell's equations on staggered grids

Erion Gjonaj [#1], Sascha Brück [##2], Thomas Weiland [#3]

[#] *TEMF, Technische Universität Darmstadt, Schloßgartenstraße 8, 64289 Darmstadt, Germany*
[##] *Integrated Systems Laboratory, ETZ J81, Gloriastr. 35, 8092 Zürich, Switzerland*
[1] gjonaj@temf.tu-darmstadt.de
[2] bruecks@iis.ee.ethz.ch
[3] thomas.weiland@temf.tu-darmstadt.de

***Abstract*—We propose a class of DG methods for the solution of Maxwell's equations in the time domain using staggered grid discretization. The method can be regarded as a generalization of the well-known FDTD technique. The present approach, however, applies to high order approximations as well. In terms of numerical properties, the method shares the energy conservation property with central flux DG formulations. On the other hand, the method is optimally convergent as is the case for dissipative DG methods using upwind fluxes. We perform a Bloch wave dispersion analysis in the one dimensional case. It shows that grid staggering allows to eliminate the spurious mode solutions originating from odd-even decoupling which are otherwise present in common DG formulations.**

I. Introduction

Discontinuous Galerkin (DG) methods provide a useful alternative to the conventional FDTD method [1] for the solution of Maxwell's equations in the time domain. Several variants have been proposed and then successfully applied in the simulation of high frequency electromagnetic field problems. Among the most prominent techniques are the nodal upwind DG method [2], the central flux DG method [3], [4], interior penalty type methods [5] and many others.

The main advantages of DG consist in the high order accuracy and in the flexible handling of unstructured grids. On the other hand, its application for electromagnetic field problems has been challenged by a number of arguments. Depending on the choice of fluxes, energy may not be conserved, as is the case for upwind type DG. In addition, the numerical solution is plagued by spurious modes. These can be roughly categorized into high frequency and low frequency solutions [2]. The former manifest themselves in the numerical dispersion relation of the method resulting in unphysical group velocities in the large wave number range of the discrete spectrum. The latter type of spurious modes is related to the violation of charge conservation and may, therefore, become apparent in the three dimensional case only [6].

It is important to note that spurious numerical solutions are absent in the conventional Yee-FDTD method. This is due to the fact that Yee's scheme operates on a pair of spatially staggered grids. Contrary to this, it is well known that applying simple central differencing on non-staggered grids will again give rise to spectral pollution by unphysical solutions; a phenomenon which is most commonly known as odd-even decoupling [7], [8]. The origin of these solutions is the same as that of the high frequency spurious modes of DG. Thus, it appears natural to seek a modified DG method using staggered grids such that at least some of the unphysical solutions of the standard approach are eliminated.

This idea has already been developed for the acoustic wave equation in two and three dimensions by Chung [9], [10] who proved stability and optimal convergence for these cases as well. The aim of the present paper is to provide a suitable formulation of the DG method on staggered grids for Maxwell's equations. Furthermore, in the paper a spatial dispersion analysis using the Bloch wave ansatz is performed which reveals the absence of spurious modes as well as the better numerical properties of the staggered grid approach compared to conventional DG formulations.

II. The DG method

We consider pure electromagnetic wave propagation problems in absence of free sources. Maxwell's equations in this case read:

$$\nabla \cdot \boldsymbol{D} = 0, \qquad \frac{\partial \boldsymbol{D}}{\partial t} - \nabla \times \boldsymbol{H} = 0, \tag{1}$$

$$\nabla \cdot \boldsymbol{B} = 0, \qquad \frac{\partial \boldsymbol{B}}{\partial t} + \nabla \times \boldsymbol{E} = 0, \tag{2}$$

where $\boldsymbol{E}$, $\boldsymbol{H}$ are the electric and magnetic field intensities, respectively, and $\boldsymbol{D}$, $\boldsymbol{B}$ the corresponding flux densities. For linear, isotropic and non-dispersive media, the flux densities are defined by constitutive relations as, $\boldsymbol{D} = \epsilon \boldsymbol{E}$ and $\boldsymbol{B} = \mu \boldsymbol{H}$, where ϵ and μ are the dielectric permittivity and magnetic permeability of the medium.

Let a partition of the computational domain, Ω, into N subdomains Ω_n (colloquially called mesh elements) be given such that $\Omega = \bigcup_{n=1}^{N} \Omega_n$. The DG method is then derived as in the standard Finite Element Method (FEM) by seeking a numerical solution of (1, 2) for the electric and magnetic field vectors in the finite dimensional approximation spaces, V_h^E

and V_h^H, respectively, in the form

$$\boldsymbol{E}_h = \sum_1^{\dim(V_h^E)} E_j \boldsymbol{\varphi}_j^E, \quad \boldsymbol{H}_h = \sum_1^{\dim(V_h^H)} H_j \boldsymbol{\varphi}_j^H, \qquad (3)$$

where $\boldsymbol{\varphi}_j^E$ and $\boldsymbol{\varphi}_j^H$ are vector basis functions in the corresponding approximation spaces. In contrast to the FEM, the DG method does not impose continuity conditions on the solution. Rather, $V_h^{E,H} = \{\boldsymbol{\varphi}_j^{E,H} \in [\boldsymbol{L}^2]^3\}$ represent discontinuous approximation spaces, where each basis function, $\boldsymbol{\varphi}_j^{E,H}$, is associated with a single mesh element, Ω_n, such that it is piecewise continuous within the element and vanishes identically outside of it. With these assumptions, the Galerkin formulation is: find $(\boldsymbol{E}_h, \boldsymbol{H}_h)$ such that

$$\int_{\Omega_n} \boldsymbol{\varphi}_i^H \mu \dot{\boldsymbol{H}}_h \mathrm{d}\Omega = -\int_{\Omega_n} \boldsymbol{E}_h \nabla\times\boldsymbol{\varphi}_i^H \mathrm{d}\Omega + \int_{\partial\Omega_n} (\boldsymbol{n}\times\boldsymbol{E}_h^*)\boldsymbol{\varphi}_i^H \mathrm{d}\Gamma,$$

$$\int_{\Omega_n} \boldsymbol{\varphi}_i^E \epsilon \dot{\boldsymbol{E}}_h \mathrm{d}\Omega = \int_{\Omega_n} \boldsymbol{H}_h \nabla\times\boldsymbol{\varphi}_i^E \mathrm{d}\Omega - \int_{\partial\Omega_n} (\boldsymbol{n}\times\boldsymbol{H}_h^*)\boldsymbol{\varphi}_i^E \mathrm{d}\Gamma,$$

$\forall \boldsymbol{\varphi}_i^E \in V_h^E$, $\forall \boldsymbol{\varphi}_i^H \in V_h^H$ and $n = 1, \ldots, N$. The formulation breaks into N blocks of equations, with each block corresponding to a subset of basis functions with compact support on a single mesh element, Ω_n. As an important consequence, the mass matrices of the DG method are block-diagonal. Thus, explicit time stepping can be applied in time domain simulations resulting in a numerically more efficient scheme than, e.g., the FEM (cf. [11] and references therein).

Since the approximations are discontinuous at element interfaces, $\partial\Omega_n$, the surface integral terms in the above equations need to be specified. A number of DG variants can be obtained by selecting different types of so called *numerical fluxes* for these terms. We recall two of them which we will need for comparison purposes in the following:

i) The central flux approach is defined by (cf. [3], [4]),

$$\boldsymbol{n} \times \boldsymbol{E}_h^* = \frac{1}{2}\boldsymbol{n} \times (\boldsymbol{E}_h^- + \boldsymbol{E}_h^+), \qquad (4)$$

$$\boldsymbol{n} \times \boldsymbol{H}_h^* = \frac{1}{2}\boldsymbol{n} \times (\boldsymbol{H}_h^- + \boldsymbol{H}_h^+), \qquad (5)$$

where $(\boldsymbol{E}_h^-, \boldsymbol{H}_h^-)$, $(\boldsymbol{E}_h^+, \boldsymbol{H}_h^+)$ are the interior and exterior field approximations at the interface $\partial\Omega_n$ of Ω_n.

ii) The upwind flux approach is [12],

$$\boldsymbol{n}\times\boldsymbol{E}_h^* = \boldsymbol{n}\times\frac{(Y^+\boldsymbol{E}_h^+ + \boldsymbol{n}\times\boldsymbol{H}_h^+) + (Y^-\boldsymbol{E}_h^- - \boldsymbol{n}\times\boldsymbol{H}_h^-)}{Y^- + Y^+}, \qquad (6)$$

$$\boldsymbol{n}\times\boldsymbol{H}_h^* = \boldsymbol{n}\times\frac{(Z^+\boldsymbol{H}_h^+ - \boldsymbol{n}\times\boldsymbol{E}_h^+) + (Z^-\boldsymbol{H}_h^- + \boldsymbol{n}\times\boldsymbol{E}_h^-)}{Z^- + Z^+}, \qquad (7)$$

where $Z = \sqrt{\mu/\epsilon}$ is the wave impedance and $Y = 1/Z$ the wave admittance of the medium.

A. Bloch wave analysis

In order to illustrate the idea, a spatial dispersion analysis is performed for the two flux approaches presented above in the one dimensional case. For the two electromagnetic field components a modal approximation with scaled Legendre polynomials as basis functions is applied (cf. [3], [4]). Then, following the derivations in [13], a Bloch wave ansatz is introduced which reduces the formulation to an eigenvalue problem in the fundamental element. The solutions of this equation provide the dispersion relation between frequency, ω, and wave number, k, for a given mesh step h.

Figure 1 shows the resulting dispersion curves in the first Brillouin zone for the central flux approach. Approximation orders $P = 0, 1, 2, 3$ are used with $P = 0$ corresponding to the lowest order case with piecewise constant basis functions. The dispersion curves form a band structure with $P+1$ bands. Each of the bands contains two branches representing the two possible propagation directions of a Bloch wave. For $P = 0$ only an acoustic band exists. For higher approximation orders, optical bands appear describing wave propagation above the Nyquist sampling limit of the grid.

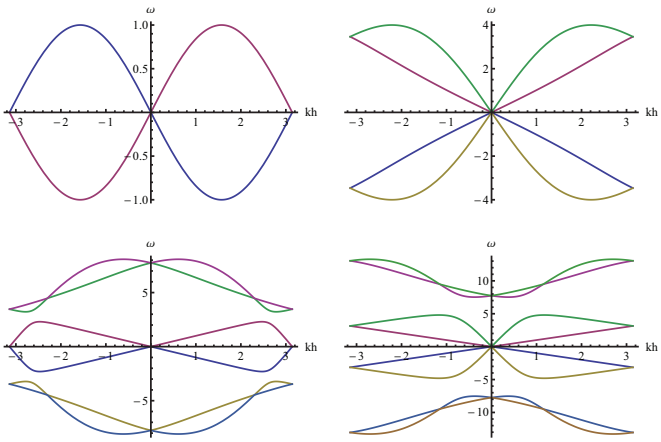

Fig. 1. Dispersion curves of the central flux DG approach for approximation orders $P = 0, 1, 2, 3$, from top-left to bottom-right, respectively.

For compactness, the dispersion curves of the upwind flux method are shown in Fig. 2 for $P = 0, 1$ only. The numerical frequencies in this case are complex. Thus, this approach is dissipative with the damping rate γ given by the imaginary part of ω. Note that the real parts of the dispersion curves for $P = 0, 1$ coincide with those of the central flux approach. This is, however, not necessarily the case for $P > 1$.

By close inspection of Fig. 1 and 2, it can be observed that the group velocity along a given dispersion branch may change sign. This is most clearly seen in both cases for $P = 0$ where, e.g., a wave propagating in the positive direction ($\omega/k > 0$) features a negative group velocity for $|hk| > \pi/2$. Another way at looking at it is the following. For every fixed frequency, the dispersion graphs predict four possible waves. Two of them describe physical propagation; the other two are spurious numerical modes. This phenomenon corresponds exactly to the odd-even decoupling which has been long known for finite difference schemes on non-staggered grids [7], [8]. The present analysis demonstrates that the same type of spurious modes appear also in the DG method. For high order approximations, the spurious modes are eventually found in the optical bands and thus shifted towards higher wave numbers. However, they

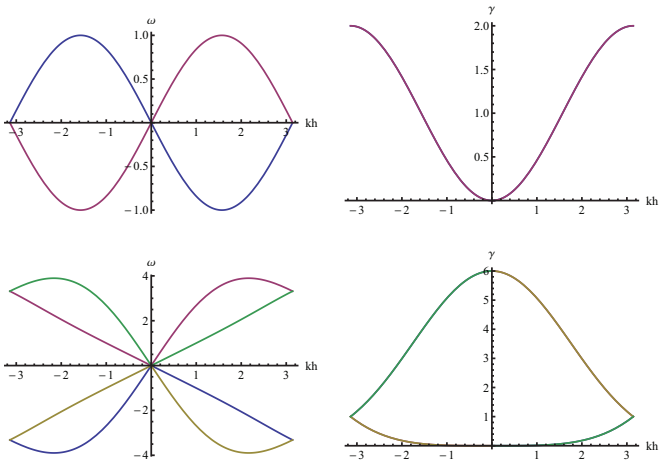

Fig. 2. Dispersion curves of the upwind flux DG approach for approximation orders $P = 0, 1$ (top $P = 0$; bottom $P = 1$).

are always present in the spectrum. In the upwind flux case, the spurious part of the spectrum is heavily damped. This can be seen as an advantage of the upwind flux approach compared to the central one. This, however, comes at the price of numerical dissipation which is not desirable in many electromagnetic field applications as well.

III. The DG method on staggered grids

Following the analogy with finite difference methods, the occurrence of odd-even decoupling can be avoided by introducing spatially staggered grids for the allocation of electric and magnetic field unknowns, respectively. For the sake of simplicity, only the one dimensional case will be considered in th following. The proposed allocation scheme is illustrated in Fig. 3. The piecewise approximation for the electric field component is sought as a piecewise continuous function within every *primary grid* cell, $\Omega_i = (x_i, x_{i+1})$, with discontinuities located at the grid nodes. The magnetic field component is approximated as a piecewise continuous function within every *dual grid* cell, $\widetilde{\Omega}_i = (x_{i-1/2}, x_{i+1/2})$, with discontinuities located at the primary cell centers.

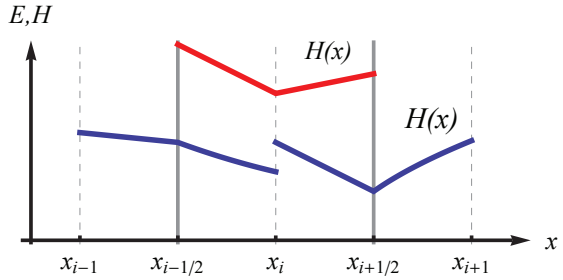

Fig. 3. Field allocation on the primary and dual cells of the staggered grid.

Note that the approximation for E in Ω_i contains a kink at the cell center, $x_{i+1/2}$, which is the exact position where the magnetic field component becomes discontinuous. Vice versa the approximation for H in $\widetilde{\Omega}_i$ kinks at x_i where E is discontinuous. This is to ensure that the regularity of the approximations is consistent with Maxwell's equations (1, 2) where electric and magnetic field components are related to each other by spatial derivatives.

A possible choice for the basis functions which generates this kind of approximation is shown in Fig. 4. In the piecewise linear case and, e.g., for the electric field component, three hat-like basis functions associated with the two nodes and with the midpoint (dual node) of the primary cell, respectively, are used. The quadratic case is obtained by adding two shifted quadratic Legendre polynomials with compact support in the left-half and right-half of the primary cell, respectively. High order complete approximations can be constructed hierarchically in a similar manner by adding higher order truncated polynomial functions with zero-crossing at the dual node in each of the two halves of the primary cell. The approximation for the magnetic field component is performed analogously in the dual grid cells. Note that, as a first consequence of the staggered grid approach, a total of $2P+1$ degrees of freedom per field component and element are required instead of the $P+1$ used in the standard DG method.

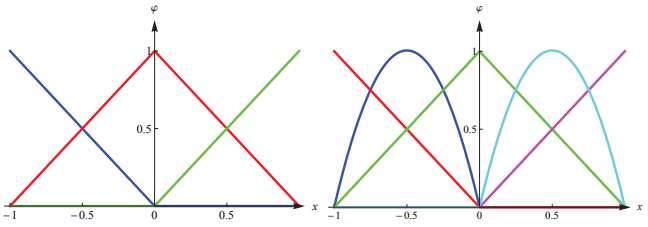

Fig. 4. Left: piecewise linear approximation in the unit cell using three hat-like nodal basis functions. Right: piecewise quadratic hierarchic approximation with five basis functions.

The Galerkin equations in the staggered grid case are,

$$\int_{\widetilde{\Omega}_n} \boldsymbol{\varphi}_i^H \mu \dot{\boldsymbol{H}}_h \mathrm{d}\Omega = -\int_{\widetilde{\Omega}_n} \boldsymbol{E}_h \nabla\times\boldsymbol{\varphi}_i^H \mathrm{d}\Omega + \int_{\partial\widetilde{\Omega}_n} (\boldsymbol{n}\times\boldsymbol{E}_h^*)\boldsymbol{\varphi}_i^H \mathrm{d}\Gamma,$$

$$\int_{\Omega_n} \boldsymbol{\varphi}_i^E \epsilon \dot{\boldsymbol{E}}_h \mathrm{d}\Omega = \int_{\Omega_n} \boldsymbol{H}_h \nabla\times\boldsymbol{\varphi}_i^E \mathrm{d}\Omega - \int_{\partial\Omega_n} (\boldsymbol{n}\times\boldsymbol{H}_h^*)\boldsymbol{\varphi}_i^E \mathrm{d}\Gamma,$$

the only difference to the standard DG method being that elemental integrals in Faraday's law are performed over dual grid cells, $\widetilde{\Omega}_n$. Since dual cell interfaces, $\partial\widetilde{\Omega}_n$, coincide with the midpoints of primary cells, the electric field there is continuous. Similarly, the magnetic field traces on primary cell interfaces, Ω_n, appearing in Ampere's law are uniquely defined. A natural choice for the numerical fluxes is then obtained by setting

$$\boldsymbol{n}\times\boldsymbol{E}_h^* = \boldsymbol{n}\times\boldsymbol{E}_h, \quad \boldsymbol{n}\times\boldsymbol{H}_h^* = \boldsymbol{n}\times\boldsymbol{H}_h. \tag{8}$$

These fluxes may be considered as a special case of (4, 5) for continuous interface fields. As in the case of DG with central fluxes, the skew-symmetric structure of Maxwell's equations is preserved. Thus, the method is conservative.

It is, however, possible to employ an upwind flux for the DG method on staggered grids as well. Using the fact that electric field components are discontinuous at primary cell interfaces

and magnetic field components are discontinuous at dual cell interfaces the Riemann solution (6, 7) takes the form

$$\boldsymbol{n}\times\boldsymbol{E}_h^* = \boldsymbol{n}\times\boldsymbol{E}_h + \boldsymbol{n}\times\boldsymbol{n}\times\frac{\boldsymbol{H}_h^+ - \boldsymbol{H}_h^-}{Y^- + Y^+}, \tag{9}$$

$$\boldsymbol{n}\times\boldsymbol{H}_h^* = \boldsymbol{n}\times\boldsymbol{H}_h - \boldsymbol{n}\times\boldsymbol{n}\times\frac{\boldsymbol{E}_h^+ - \boldsymbol{E}_h^-}{Z^- + Z^+}. \tag{10}$$

This approach, obviously, results in a dissipative scheme since it includes in the formulation penalty terms involving the tangential field jumps at element interfaces.

A one dimensional Bloch wave analysis can be performed analogously to the standard method. For this purpose, only the conservative scheme with fluxes defined in (8) will be considered. Figure 5 shows the resulting spatial dispersion curves in the first Brillouin zone for $P = 0, 1, 2, 3$. Again a band structure is obtained with pairs of dispersion branches corresponding to plane waves propagating in the positive and negative directions, respectively.

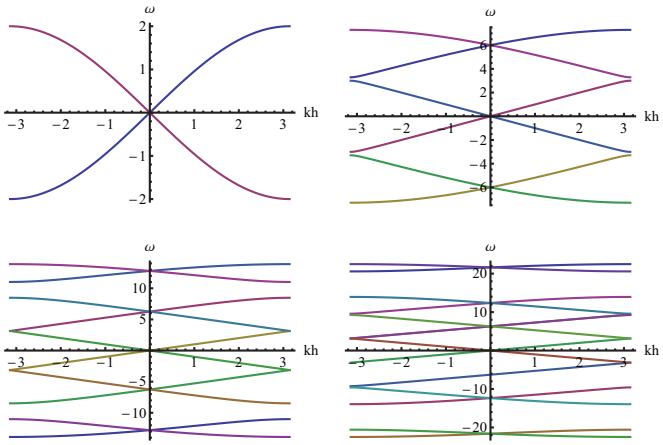

Fig. 5. Dispersion curves of the DG method on staggered grids using the conservative fluxes (8) for approximation orders $P = 0, 1, 2, 3$ from top-left to bottom-right, respectively.

A number of important observations can be made. First, the dispersion curves for a piecewise constant approximation are identical with those of the FDTD method. In fact, the two methods are algebraically equivalent. Thus, the FDTD method can be considered as special case of DG on staggered grids for lowest order approximation with $P = 0$.

Second, all dispersion branches represent monotonic functions of frequency vs. wave number. Thus, group and phase velocities point in the same direction. In other words, for every frequency solution there exist exactly two waves propagating in opposite directions. Therefore, the DG method on staggered grids does not support spurious modes resulting from odd-even decoupling as is the case for non-staggered DG.

Third, the spectral range for plane wave solutions, in terms of the scaled wave number, is $hk \in [-(2P+1)\pi, (2P+1)\pi]$ as compared to $hk \in [-(P+1)\pi, (P+1)\pi]$ for non-staggered DG. Thus, the DG method on staggered grids can handle shorter wave length solutions for the same mesh step, h. This is a direct consequence of the larger number of degrees of freedom used in the formulation.

Finally, the staggered grid approach shows a substantially smaller dispersion error than the two standard DG methods. This can be more easily observed in the $P = 0$ case for wave numbers close to the grid sampling limit. As can be seen in Fig. 1 and 2, the phase velocity in the non-staggered case drops to zero for $hk = \pm\pi$. In the staggered grid case (cf. Fig. 5), the phase error is much smaller, even at the cut-off wave number where it reaches its maximum.

IV. Conclusions

A high order DG method on staggered grids for Maxwell's equations is introduced. The scheme is constructed by applying a special approximation with piecewise continuous basis functions defined in the primary and dual grid cells, respectively. We have investigated the properties of the method in the one dimensional case from the point of view of numerical dispersion using Bloch wave analysis. It shows that the staggered grid approach allows to eliminate spurious solutions resulting from odd-even decoupling. The method is more accurate than conventional DG. This, however, comes at the price of a larger number of degrees of freedom which is required by construction in the staggered grid formulation.

References

[1] Kane Yee, Numerical solution of initial boundary value problems involving Maxwell's equations in isotropic media, IEEE Transactions on Antennas and Propagation 14 (3): 302–307 (1966).

[2] J. S. Hesthaven and T. Warburton, Nodal High–Order Methods on Unstructured Grids: I. Time–Domain Solution of Maxwell's Equations, Journal of Computational Physics 181: 186–221 (2002).

[3] L. Fezoui, S. Lanteri, S. Lohrengel and S. Piperno, Convergence and stability of a Discontinuous Galerkin time–domain method for the 3D heterogeneous Maxwell equations on unstructured meshes, ESAIM: Math. Model. and Numer. Anal. 39: 1149–1176 (2005).

[4] E. Gjonaj, T. Lau, S. Schnepp, F. Wolfheimer, and T. Weiland. Accurate modelling of charged particle beams in linear accelerators. New Journal of Physics, 8(11):285 (2006).

[5] M. J. Grote, A. Schneebeli, D. Schotzau, Interior penalty discontinuous Galerkin method for Maxwell's equations, J. Compu. Appl. Math. , vol. 204: 375–386 (2007).

[6] E. Gjonaj, T. Lau and T. Weiland, Conservation Properties of the Discontinuous Galerkin Method for Maxwell Equations, International Conference on Electromagnetics in Advanced Applications (ICAA 2007), Torino, Italy, September 2007, pp. 356–359.

[7] D.R. Lynch and K.D. Paulsen, Origins of vector parasites in numerical Maxwell solutions, IEEE Trans. Microwave Theory Tech. 39, 383394 (1991).

[8] L. N. Trefethen, Group Velocity in Finite Difference Schemes, SIAM Review 24: 113–136 (1982).

[9] E. T. Chung and B. Engquist, Optimal discontinuous Galerkin methods for wave propagation, SIAM J. Numer. Anal. 44: 2131–2158 (2006).

[10] E. T. Chung and B. Engquist, Optimal discontinuous Galerkin methods for the acoustic wave equation in higher dimensions, SIAM J. Numer. Anal. 47: 3820–3848 (2009).

[11] J.S. Hesthaven and T. Warburton, Nodal Discontinuous Galerkin Methods: Algorithms, Analysis, and Applications. Springer Texts in Applied Mathematics 54. Springer Verlag, New York, 2008.

[12] A. H. Mohammadian, V. Shankar and W. F. Hall, Computation of electromagnetic scattering and radiation using a time–domain finite–volume discretization procedure, Comput. Phys. Comm. 68: 175–196 (1991).

[13] M. Ainsworth, Dispersive and dissipative behaviour of high order discontinuous Galerkin finite element methods, Journal of Computational Physics 198: 106–130 (2004).